

Simulation of microstructures in solidification of aluminum twin-roll casting based on CA

LIU Xiao-bo(刘晓波)¹, XU Qing-yan(许庆彦)², JING Tao(荆涛)², LIU Bai-cheng(柳百成)²

1. School of Aeronautics and Mechanical Engineering, Nanchang Hangkong University, Nanchang 330063, China;
2. Department of Mechanical Engineering, Tsinghua University, Beijing 100084, China

Received 12 November 2008; accepted 7 January 2009

Abstract: The microstructures in the solidification process of aluminum twin-roll casting was simulated based on CA (Cellular Automaton Method), and the nucleation model based on the normal distribution and KUZR-GIOVANOLS-TRIVEDI(KGT) growth model were used in the calculation. FDM (Finite Difference Method) combined with relative motion was used, and dynamic evolution of microstructures in the process of aluminum twin-roll casting was achieved. Visual Fortran programming language was adopted to calculate and realize the image post-processing. Moreover, the effect of different casting process parameters on the formation of the microstructures was simulated. The results are helpful to explaining the dendritic segregation and size segregation as well as shrinkage-porosity defects. Columnar grains mainly distribute near the casting roller while equiaxed grains distributed far away from the casting roller.

Key words: Cellular Automaton; microstructure; numerical simulation; twin-roll casting

1 Introduction

By the simulation of the microstructure in aluminum twin-roll casting process[1–2], which can forecast the microstructure growth and the performances of aluminum strip with a small amount of work, we can obtain the quantitative relationship between major process parameters and solidification microstructure. So it provides a theoretical basis to optimize aluminum casting process and quality control.

With the continuous development of computing technology, all kinds of simulation methods have appeared. The main methods are deterministic method, stochastic method and phase-field method. The mass conservation equation in the solidification process and nucleation growth model can be coupled by deterministic simulation, and in consideration of the macro-segregation and solid transmission, it is closer to the actual solidification process. But some random phenomena in the process of grain growth cannot be treated, so it is difficult to simulate the dendrite growth

and morphology in solidification process[3–5]. Unified control equation was used in phase field method, which is unnecessary to distinguish solid-liquid phase and to track the solid/liquid interface[6–15]. It has unique advantages in simulating three-dimensional grain growth but with large amount of computation, low efficiency and small computational domain, which is difficult for simulating actual roll casting process. While stochastic simulation can couple the energy equation and nuclear-growth model, which is better to describe the formation of columnar grains and the transition from columnar grains to equiaxed grains. The two main methods including MC (Monte Carlo) method and CA (Cellular Automaton) are more representative among the stochastic methods. Though grain microstructure similar to the actual casting microstructures can be got by MC method, it is lack of physical infrastructure. CA law was initially used to simulate the grain growth of recrystallization, and later it was introduced to simulate the formation of the grain in the solidification process by RAPPAZ and GANDIN[16–17]. Based on physical mechanism of nucleation process and kinetics of grain

growth, the size and distribution of grain can be got, and the formation of columnar grains and the conversion from columnar grains to equiaxed grains can also be described by CA[18–25]. In the present work, the microstructure of aluminum strip in the casting solidification process was simulated by CA and the influence of different casting process parameters on the formation of the microstructures was studied.

2 Mathematical model

2.1 Nucleation model

Continuous nucleation model that was heterogeneous nucleation based on Gaussian distribution was used. Assume that nucleation occurs at different positions, and these nucleation locations can be described by continuous rather than discrete distribution function $dn/d(\Delta T)$. The density of grains $n(\Delta T)$ at a given degree of super-cooling ΔT is given by the integral of nucleation density distribution:

$$n(\Delta T) = \int_0^{\Delta T} \frac{dn}{d(\Delta T')} d(\Delta T') \quad (1)$$

$$\frac{dn}{d(\Delta T)} = \frac{n_{\max}}{\sqrt{2\pi}\Delta T_{\sigma}} \exp\left[-\frac{1}{2}\left(\frac{\Delta T' - \Delta T_N}{\Delta T_{\sigma}}\right)^2\right] \quad (2)$$

where $\Delta T'$ is the degree of super-cooling; ΔT_N is the mean nucleation degree of super-cooling; ΔT_{σ} is the standard curvature degree of super-cooling and n_{\max} is the total density of grains.

2.2 Growth model

Grain growth is related not only to the steady growth of dendrite tip, but also to the continuous generation and evolution of non-steady-state branching structure. Under the mobile coordinates with solid/liquid interface as the origin, when interface moves along the normal direction at speed v , the temperature and solute field in the front of the interface can be given as follows:

$$\alpha_L \Delta^2 T + v \frac{\partial T}{\partial n} = 0 \quad (3)$$

$$D_L \Delta^2 C + v \frac{\partial C}{\partial n} = 0 \quad (4)$$

where T is the temperature of the alloy; C is the concentration of the alloy; D_L is the diffusion coefficient of the liquid phase; and α_L is the heat diffusion coefficient.

But the growth velocity v and radius R of the dendrite tip cannot be achieved through this relationship. LANGER and MULLER-KRUMBNAAR[26] served $R=\lambda_C$ as a constraint condition under the interface stability theory, where λ_C is the minimum critical

disturbance wavelength.

$$\sigma^* m_L G_C \xi_C - G = \frac{\Gamma}{\sigma^* R^2} \quad (5)$$

where m_L is the slope of liquidus; G_C is the compositional gradient of interface; ξ_C is the function of Peclet number; G is the average temperature gradient; σ^* is the stability constant, $\sigma^*=1/(4\pi^2)$; Γ is the Gibbs-Thomson coefficient; and R is the growing radius of dendrite tip.

Degree of super-cooling, ΔT , is composed of four parts:

$$\Delta T = \Delta T_C + \Delta T_R + \Delta T_T + \Delta T_K \quad (6)$$

where ΔT_C is the ingredient degree of super-cooling; ΔT_R is the curvature degree of super-cooling; ΔT_T is the thermal degree of super-cooling; and ΔT_K is the kinetics degree of super-cooling.

The twin-roll casting process is a sub-rapid solidification with the nature of directional solidification. Grain growth velocity is not very highly relative to rapid solidification. The kinetic coefficient of alloys is great. The kinetic degree of super-cooling of dendrite tip can be neglected. And as the solidification undergoes in the quasi-equilibrium condition, it can be deemed that the balanced distribution coefficient remains unchanged. Therefore, this model can be amended, which can be seen as follows:

$$\Delta T = \Delta T_C + \Delta T_R \quad (7)$$

$$\Delta T_C = m_L C_0 \left[1 - \frac{1}{1 - (1 - K_0) I\nu(Pe)} \right] \quad (8)$$

$$\Delta T_R = K \frac{\sigma}{\Delta S_f} = \frac{2\Gamma}{R} \quad (9)$$

where C_0 is the initial concentration of the alloy; K_0 is the initial curvature of interface; σ is the surface energy; ΔS_f is the entropy of volume's melting; Pe is the Peclet number of solute; and $I\nu(Pe)$ is the Ivantsov function of Peclet number.

The growth radius R of dendrite tip can be attained according to the minimum critical wavelength criterion as Eq.(5):

$$R = \sqrt{\frac{\Gamma}{\sigma^* (m_L G_C \xi_C - G)}} \quad (10)$$

As $Pe=VR/2D_L$, a unitary quadratic equation about v can be got as

$$v^2 \left(\frac{\pi^2 \Gamma}{Pe^2 D_L^2} \right) + v \left\{ \frac{m_L C_0 (1 - K_0)}{D_L [1 - (1 - K_0) I\nu(Pe)]} \right\} + G = 0 \quad (11)$$

When Pe is given, the velocity v can be attained. KGT is used as the growth model.

3 Numerical calculation method

3.1 Computing model

Fig.1 shows the schematic diagram of aluminum twin-roll casting. For the size of the width direction is larger than that of the thickness direction, two-dimensional model can be applied in the simulation. Fig.1 shows that the calculation region in casting solidification process is symmetrical. In order to save the computing time, it can be calculated by half interception in accordance with its symmetry. In the application of Cellular Automation method, the formation of microstructure was simulated by the finite difference method. A simplified model in Fig.2 was used. A state array $m \times n$ in Fig.2 was used to record the state of every cell, and the coordinate of any spot can be expressed by (i, j) . In Table 1, we can clearly see the relationship between the state value of cell and the corresponding state.

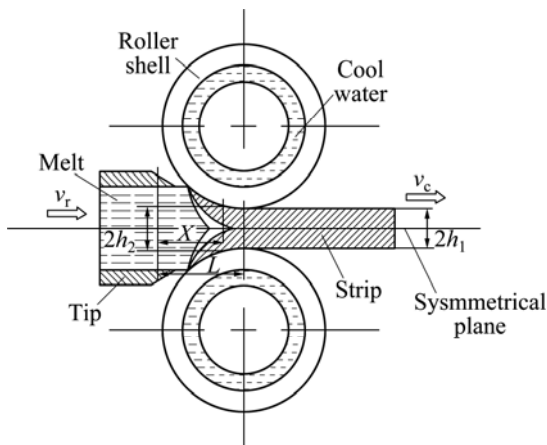


Fig.1 Schematic diagram of aluminum twin-roll casting

The microstructure formation process comes with the changes of solid-phase fraction $\Delta f_s(i, j)$. Two arrays $m \times n$ can be used to express the solid-phase fraction $f_s(i, j)$ of each cell and its increment $\Delta f_s(i, j)$. With the formation of microstructure, f_s of some cells continues to increase, then turns into solid state when $f_s(i, j) \geq 1$. Microstructure formation and dynamic evolution can be described through the changes of cellular state. As the composition gradient exists between equi-liquid phase components of interface and those away from the inter-

face, it will rule out extra solute and move forward. If the distance between the spot (i, j) and $(a, h+r)$ satisfies the following condition, the spot (i, j) can be deemed as a cell in calculating domain:

$$\sqrt{(a - i\Delta X)^2 + (h + r - j\Delta X)^2} \geq r \tag{12}$$

where a is the casting length; $2h$ is the thickness of the aluminum strip export; r is the radius of casting roll; and ΔX is the side length of square cell.

According to the geometric relations: $m=a/\Delta X$, $n=(r+h-\sqrt{r^2-a^2})/\Delta X$, since m, n are rounded, input parameters such as a, r and h in the input interface of programming are enough.

3.2 Finite difference equations

Mass conservation equation is

$$\frac{\partial C_L}{\partial t} = D_L \left(\frac{\partial^2 C_L}{\partial X^2} + \frac{\partial^2 C_L}{\partial Y^2} \right) \tag{13}$$

After a finite difference, there is

$$C_L^{t+\Delta t}(i, j) = fC_L^t(i+1, j) + fC_L^t(i-1, j) + fC_L^t(i, j-1) + fC_L^t(i, j+1) + (1-4f)C_L^t(i, j) \tag{14}$$

where t is time; Δt is time-step; $f=D_L\Delta t/(\Delta X)^2$.

While

$$\Delta t < \min \left(\frac{\Delta X^2}{4D_L}, \frac{\Delta X}{V_{\max}} \right) \tag{15}$$

Energy conservation equation is

$$\rho c_p \frac{\partial T}{\partial t} = \lambda \left(\frac{\partial^2 T}{\partial X^2} + \frac{\partial^2 T}{\partial Y^2} \right) + \rho L \frac{\partial f_s}{\partial t} \tag{16}$$

After a finite difference, there is

$$T^{t+\Delta t}(i, j) = gT^t(i-1, j) + gT^t(i+1, j) + gT^t(i, j-1) + gT^t(i, j+1) + (1-4g)T^t(i, j) + (L/c_p)\Delta f_s(i, j) \tag{17}$$

where $g=\lambda\Delta t/[\rho c_p(\Delta X)^2]$; f_s means solid-phase friction; and Δf_s means the increment of solid-phase friction.

$$T^{t+\Delta t}(i, j) - T^t(i, j) > \Delta T_N \tag{18}$$

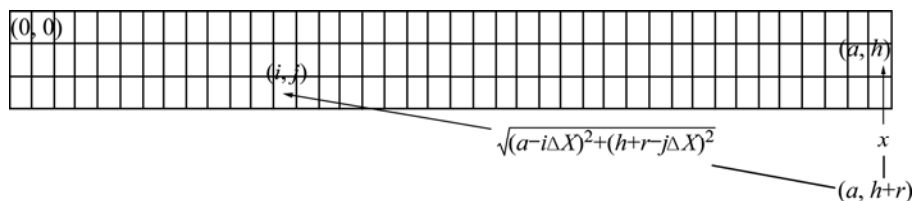


Fig.2 Calculation method of capturing cells

Table 1 Relationship between state value of cell and corresponding state

State value	0	(0, 1)	1
Corresponding state	Liquid	Mushy	Solid

3.3 Treatment of relative motion

In the casting solidification process, as aluminum strip moves with the casting roll, it is a dynamic process. Here relative movement as a simple approach was used for processing. Under the influence of casting speed U , the grains are less and growth time is shorter when it is apart from the casting mouth, while the growth time is relatively longer at export of aluminum strip. Assume the distance between a grain and the entrance to aluminum strip is expressed as L , the time of nucleation and growth L/U will be figured out easily. There is a sequence between grain nucleation and growth in the whole numerical simulation on microstructure. Because there is a direct relationship between the random nucleation and temperature field, the cell begins to nuclear at random when the temperature of the cell is lower than that of the liquidus and the degree of super-cooling of nucleation is larger. Therefore, the order of the nucleation can be controlled by calculating the temperature field. At the export of aluminum strip, with the increase of growth time, the computational domain moves constantly to entrance. If $t < a/v$, the computational domain is vt in the horizontal direction; otherwise, it keeps the same.

Some parameters used in the calculation are listed in Table 2.

Table 2 Partial thermophysical properties used in simulation

Thermal conductivity, $\lambda/(W \cdot m^{-1} \cdot ^\circ C^{-1})$	Specific heat, $c_p/(J \cdot m^{-3} \cdot ^\circ C^{-1})$	Latent heat, $L_p/(J \cdot m^{-3})$
241	2.96×10^6	9.5×10^8
Liquidus, $T_L/^\circ C$	Solidus, $T_S/^\circ C$	Partition coefficient, k
659	615	0.117

4 Simulation results and analysis

In the numerical simulation of aluminum casting solidification process, Fortran programming language was used to calculate and realize the image post-processing, that is, updating an image in each time step to achieve the dynamic evolution of microstructure nucleation and growth. A number of problems in the formation of the microstructure can also be found timely, and a lot of time was saved for debugging procedures.

The calculating domain is as follows: the width of the access point is 3.1 mm, the width of the export is 1 mm, the length is 50 mm, and the calculating domain is divided into 8.508×10^7 cells with a cell size of $1 \mu m \times$

$1 \mu m$. Fig.3 shows the simulation results of microstructures.

From Figs.3(a) and (b), it can be seen that nucleation and growth of the microstructure in export takes precedence over that in entrance, that is to say, the microstructure nucleates and grows from the exit to the entrance of aluminum strip. It can be seen from Fig.3(c) that it is clear to distinguish solid, liquid and solid-liquid phase well. From Fig.3(b), it can be seen that columnar grains are distributed adjacent to casting roll, while equiaxed grains are distributed far from casting roll, which is consistent with the theoretical analysis. It can also be clearly seen that there are many wine small molten pools in solid phase, which indicates that the solute concentration of these small molten pools is high, so segregation will appear after complete solidification. Small-scale isolate liquid region in inter-dendrite may be formed in dendrite growth. When the partition coefficient is less than 1, the liquid solute concentration in isolated region is higher than that in the surrounding region, which produces dendritic segregation and size segregation after complete solidification. When the contraction coefficient of solidification is larger, it may produce shrinkage-porosity defects. We can come to a conclusion that simulation is helpful to explaining the root causes of deficiencies in the microstructure theoretically.

From Figs.3(b–d), it can be seen that the time of nucleation and growth is relatively shorter in the entrance while longer in the export of aluminum strip. The time difference can be calculated by $t=a/v$. The greater the speed, the shorter the time. The time of nucleation and growth of microstructure in the export is also shorter, which may result in the fact that many remnants of molten aluminum will not solidify in the roll casting process, then affecting aluminum processing performance. When the speed is slower, the roughcast of aluminum strip that hasn't yet arrived the export has been fully solidified, so the casting roll will overcome the deformation in casting process, which will consume more energy. From Figs.3(b), (e) and (f), it can be seen that the greater the inner-cooling intensity, the greater the degree of super-cooling. It begins to nuclear when the temperature of the cellular is lower than that of the liquidus, the cooling is larger than degree of super-cooling of nucleation, and the nucleation rate increases greatly. When the inner-cooling intensity is small, there will be many remnants of molten aluminum in the casting process, affecting the quality of aluminum strip. While when it is large, the roughcast of aluminum strip that hasn't yet arrived the export has been fully solidified, which will consume more energy in the slower speed. Therefore, all casting process parameters should

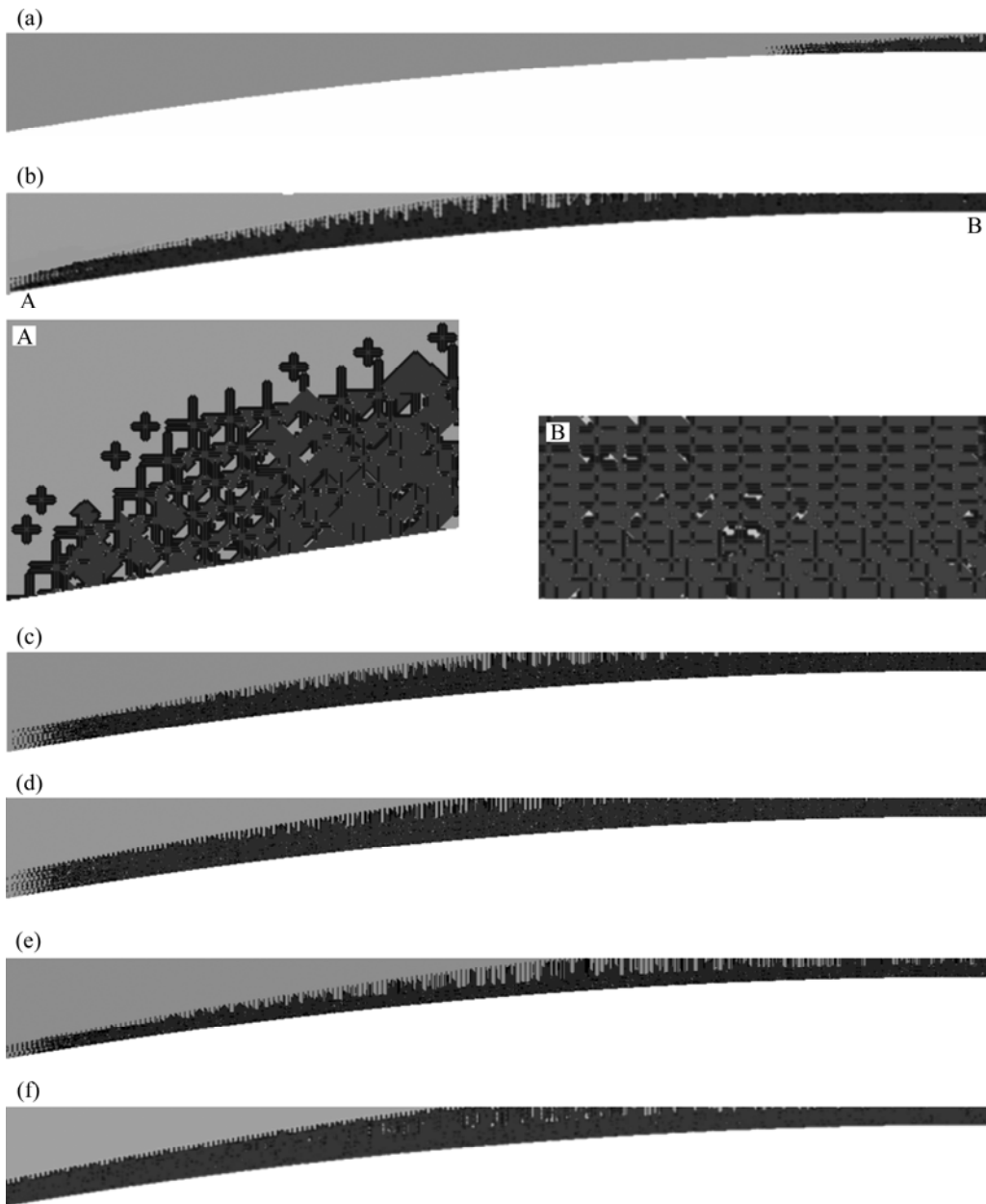


Fig.3 Simulation results of microstructures of aluminum casting solidification process: (a) Inner-cooling intensity $10 \text{ kW}/(\text{m}^2 \cdot ^\circ\text{C})$, casting speed 0.1 m/s , time 0.142 s ; (b) Inner-cooling intensity $10 \text{ kW}/(\text{m}^2 \cdot ^\circ\text{C})$, casting speed 0.1 m/s , time 0.5 s ; (c) Inner-cooling intensity $10 \text{ kW}/(\text{m}^2 \cdot ^\circ\text{C})$, casting speed 0.067 m/s ; (d) Inner-cooling intensity $10 \text{ kW}/(\text{m}^2 \cdot ^\circ\text{C})$, casting speed 0.033 m/s ; (e) Inner-cooling intensity $5 \text{ kW}/(\text{m}^2 \cdot ^\circ\text{C})$, casting speed 0.1 m/s ; (f) Inner-cooling intensity $15 \text{ kW}/(\text{m}^2 \cdot ^\circ\text{C})$, casting speed 0.1 m/s

be considered to optimize the casting solidification process.

5 Conclusions

1) Nucleation model and KGT growth model of microstructure based on CA was provided to a finite-difference calculation on the temperature field and solute field in the casting solidification process of aluminum strip, and the dynamic process of constantly pushing forward was dealt with a relative motion flexibly.

2) Fortran programming language was used to

calculate and realize the image post-processing, that is, updating an image in each time step to achieve the dynamic evolution of nucleation and growth of the microstructure.

3) It was clear to distinguish the solid, liquid and solid-liquid phase well through simulation. The transition from columnar grains to equiaxed grains was simulated that columnar grains were distributed adjacent to casting roll, while equiaxed grains were distributed far from casting roll.

4) The formation of microstructures of aluminum strip in casting solidification process was simulated,

which was helpful to explaining the root causes of deficiencies such as dendritic segregation, size segregation and shrinkage-porosity in the microstructure theoretically.

5) The influence of different casting process parameters on the formation of microstructures was simulated. The faster the casting speed and the smaller the inner-cooling intensity, the more difficult for complete solidification in the export, which would affect the quality of aluminum strip. While the speed is slower and the inner-cooling intensity is greater, it starts to solidify far from the export, which consumed more energy in the rolling process and would affect aluminum processing performance.

References

- [1] LIU Bai-cheng, JING Tao. Casting engineering simulation and quality control [M]. Beijing: China Machine Press, 2001: 4–8. (in Chinese)
- [2] SPITTLE J A, BROWN S G R. Computer simulation of the effects of alloy variables on the grain structure of castings [J]. *Acta Metall*, 1989, 37(7): 1803–1810.
- [3] WANG Y C, BECKRMANN C. Multi-scale/-phase modeling of dendritic alloy solidification, transport phenomena in solidification [J]. *ASME Heat Transfer Division*, 1994, 284: 75–95.
- [4] BROWN D J, HUNT J D. A model of columnar growth using a front-tracking technique [C]// *Modeling of Casting, Welding and Advanced Solidification Processes XI*. Aachen, Germany, 2000: 437–444.
- [5] MA Chang-wen, SHEN Hou-fa, HUANG Tian-you, LIU Bai-cheng. Numerical simulation of macro-segregation with equiaxed grains movement [J]. *Chinese Journal of Materials Research*, 2004, 18(3): 232–238. (in Chinese)
- [6] DIEPERS H J, BECKRMANN C, STEINBACH I. Simulation of convection and ripening in a binary alloy much using the phase field method [J]. *Acta Mater*, 1999, 47(3): 3663–3678.
- [7] GEORGE W L, WARREN J A. A parallel 3D dendritic growth simulator using the phase-field method [J]. *Journal of Computational Physics*, 2002, 177: 264–283.
- [8] ZHANG G Y, JING T, LIU B C. Microstructure simulation of aluminum alloy casting using phase field method [J]. *Int J Cast Metal Res*, 2002, 15(13): 237–240.
- [9] ZHU Chang-sheng, WANG Zhi-ping, JING Tao, LIU Bai-cheng. Phase-field simulation of dendritic sidebranching induced by thermal noise [J]. *Trans Nonferrous Met Soc China*, 2004, 14(6): 1106–1110.
- [10] GUO Jin-jie, LI Xin-zhong, SU Yan-qing. Phase field simulation of structure evolution at high growth velocities during directional solidification of Ti55 Al45 alloy [J]. *Intermetallics*, 2005, 13: 275–279.
- [11] ZHU Yao-chan, YANG Gen-cang, WANG Jin-cheng, ZHAO Da-wen, FAN Jian-feng. Multi-phase field simulation of uni-directional solidification for binary eutectic alloys [J]. *The Chinese Journal Nonferrous Metals*, 2005, 15(7): 1026–1032. (in Chinese)
- [12] LI Xin-zhong, GUO Jing-jie, SU Yan-qing, WU Shi-ping, FU Heng-zhi. Phase-field simulation of dendritic growth for binary alloys with complicate solution models [J]. *Trans Nonferrous Met Soc China*, 2005, 15(4): 769–776.
- [13] ZHAO Hong-zhao, JING Tao, LIU Bai-cheng. Simulation of 3-D dendritic growth of aluminum alloy by phase field model [J]. *Acta Metall Sinica*, 2005, 41(5): 491–495. (in Chinese)
- [14] LI Mei-e, YANG Gen-cang, ZHOU Yao-he. Phase field modeling of directional solidification of a binary alloy at high velocities [J]. *Acta Phy Sinica*, 2005, 54(1): 454–459. (in Chinese)
- [15] YANG Yu-juan, WANG Jin-cheng, ZHU Yao-chan, ZHANG Yu-xiang, YANG Gen-cang. Multi-phase field simulation of isothermal free binary eutectic growth [J]. *Rare Metal Mater and Eng*, 2007, 36(4): 573–577. (in Chinese)
- [16] RAPPAPAZ M, GANDIN C A. Probabilistic modeling of microstructure formation in solidification process [J]. *Acta Metall*, 1993, 41(2): 345–360.
- [17] GANDIN C A, RAPPAPAZ M. Coupled finite element-cellular automaton model for the prediction of dendritic grain structures in solidification process [J]. *Acta Metall*, 1994, 42(7): 2233–2246.
- [18] NASTAC L. Numerical modeling of solidification morphologies and segregation patterns in cast dendritic alloys [J]. *Acta Meter*, 1999, 47(17): 4253–4262.
- [19] BELTERAN-SANCHEZ L, STEFANESCU D M. A quantitative dendrite growth model and analysis of stability concepts [J]. *Metall Mater Trans A*, 2004, 35A(8): 2471–2485.
- [20] ZHU M F, LEE S Y, HONG C P. Modified cellular automaton model for the prediction of dendritic growth with melt convection [J]. *Phys Rev E*, 2004, 69(61): 061610–1–061610–12.
- [21] XU Qing-yan, FENG Wei-ming, LIU Bai-cheng. Coupled macro-micro modeling for prediction of grain structure of Al alloy [J]. *Trans Nonferrous Met Soc China*, 2004, 14(1): 71–77.
- [22] KANG Xiu-hong, DU Qiang, LI Dian-zhong, LI Yi-yi. Modeling of the solidification by coupling Cellular Automaton with macro-transport model [J]. *Acta Metall Sinica*, 2004, 40(5): 452–456. (in Chinese)
- [23] CHEN Jin, ZHU Ming-fang, SUN Guo-xiong. Numerical simulation on free dendrite growth in undercooled melt using using Cellular Automaton method [J]. *Acta Metall Sinica*, 2005, 41(5): 799–803. (in Chinese)
- [24] WANG Kuang-fei, LI Bang-sheng, MI Guo-fa, GUO Jing-jie, FU Heng-zhi. Numerical simulation of cellular/dendrite transition and its growth during direction solidification of Ti44Al alloy [J]. *Acta Metall Sinica*, 2007, 43(2): 211–216. (in Chinese)
- [25] LIU Xiao-bo, XU Qing-yan, JING Tao, LIU Bai-cheng. Research on microstructure of aluminum twin-roll casting based on Cellular Automation [J]. *Trans Nonferrous Met Soc China*, 2008, 18(4): 944–948.
- [26] LANGER J S, MULLER-KRUMBNAAR H. Stability effects in dendritic crystal growth [J]. *Journal of Cryst Growth*, 1977, 42: 11–14.

(Edited by YANG Bing)